Fang *et al. Applied Biological Chemistry* (2022) 65:46
https://doi.org/10.1186/s13765-022-00715-9

KSABC
The Korean Society for Applied Biological Chemistry

ARTICLE Open Access

Depressing hsa_circ_0058092 functions an integrated anti-proliferation and anti-motility role in gastric cancer partially through targeting miR-1294/SIX1 axis

Jianming Fang, Jianxin Huang and Xiaodong Zhang*

Abstract

Fibronectin 1-derived circular RNA hsa_circ_0058092 is a novel potential oncogene in gastric cancer (GC). Yet, previous studies have not determined the role of hsa_circ_0058092 GC progression and the underlying mechanism. Herein, we investigated its role and competing endogenous RNA (ceRNA) pathway in the development of GC. The results showed that hsa_circ_0058092 was substantially upregulated in GC patients' tissues and cells, allied with upregulated SIX1 and downregulated miR-1294 compared with normal gastric tissues and cells. There were linear correlations among hsa_circ_0058092, miR-1294 and SIX1 levels in GC tumors. Moreover, hsa_circ_0058092 acted as a miR-1294 sponge, and miR-1294 targeted SIX1. Functionally, colony formation, EdU positive rate, tumor growth of GC cells, as well as ki-67 expression in xenograft tumors was greatly suppressed by depressing hsa_circ_0058092. Besides, hsa_circ_0058092 knockdown repressed GC cell migration and invasion, accompanied with increased E-cadherin expression and descended N-cadherin expression. Moreover, inhibiting miR-1294 expression could counteract hsa_circ_0058092 knockdown-mediated effects in GC cells. The inhibitory effects of miR-1294 mimics on GC cell malignancy were relieved by increasing SIX1 expression. Further, hsa_circ_0058092 depletion repressed SIX1 protein expression by interacting with miR-1294. Hsa_circ_0058092 was oncogenic in GC cell proliferation and motility via ceRNA pathway of hsa_circ_0058092/miR-1294/SIX1.

Keywords: Hsa_circ_0058092, miR-1294, SIX1, Gastric cancer

Introduction

Gastric cancer (GC) is one of the top common cancers and primary risks of cancer-related deaths [1]. Patients with early stage of GC are usually symptom-free [2], and endoscopy combines with biopsy is the golden standard for the diagnosis of GC [3]; however, endoscopic biopsy is an invasive method and is difficult for mass screening; sometimes it has complications such as bleeding and perforation [4]. In this scenario, it is essential to find new potential minimally invasive biomarker for early diagnosis of GC.

Circular RNAs (circRNAs) are a special class of endogenous noncoding and coding RNAs with a closed-loop structure [5, 6]. In very recent years, circRNA research has been emerging and booming in human diseases, especially in cancer [7]. In GC, circRNAs are reviewed as new regulators for diagnosis and cancer therapy [8], and their biogenesis, functional role and clinical significance have been systematically summarized [9]. Moreover, some circulating molecules including circRNAs, microRNAs (miRNAs) and messenger RNAs (mRNAs) in body fluids have been recently discovered in the screening and early diagnosis of GC [10]. For example, fibronectin 1

*Correspondence: Lecter2009@163.com

Hepatobiliary and Pancreatic Surgery, Zhejiang Jinhua Guangfu Tumor Hospital, No. 1296, North huancheng Road, Jinhua 321000, China

(FN1) is one of hub genes that are differently expressed and can predict poor prognosis in GC [11]. Besides, FN1 is associated with protein–protein interaction network and circRNA-miRNA-mRNA network [12]. MiR-339-5p inhibited GC cell proliferation and migration through alkB homolog 1, histone H2A dioxygenase (ALKBH1) [13]. MiR-216b combined with paxillin (PXN) to repress GC cell proliferation and metastasis [14]. Next generation sequencing (NGS) is an emerging trend in molecular biology of GC [15], and the circRNA expression profile in GC patients' tissues has been established [16]. In particular, circ_0004872 [17] and circ-TNPO3 [18] inhibited GC cell malignant progression and circ_0008035 [19] had the opposite effect.

FN1-derived circRNA hsa_circ_0058092 is suggested to be a potential oncogene in GC via sponging miRNA (miR)-4269 and regulating a broad-spectrum prognostic biomarker protein [16, 20]. According to three bioinformatics algorithms, miR-1294 is a novel and promising candidate target for hsa_circ_0058092, and miR-1294 is a risk factor for the diagnosis and prognosis of GC [21]. However, the interaction between hsa_circ_0058092 and miR-1294 remains to be further validated. Furthermore, the critical homeobox transcription factor sine oculis homeobox homolog 1 (SIX1) is an independent biomarker in tumorigenesis including GC [22, 23]. Whilst, it is unclear that whether there is a hsa_circ_0058092/miR-1294/SIX1 axis in regulation of GC malignant behaviors.

Therefore, in this study, we aimed to analyze the role of hsa_circ_0058092 in GC progression and the underlying mechanism. We first investigated the expression of hsa_circ_0058092, miR-1294 and SIX1 in GC tissues cells and identified whether miR-1294 bound to hsa_circ_0058092 and SIX1. Subsequently, we determined whether hsa_circ_0058092 regulated GC cell processes through miR-1294, and whether miR-1294 mediated GC cell malignancy by associating with SIX1. Eventually, this work analyzed whether hsa_circ_0058092 modulated SIX1 expression in a miR-1294-dependent manner.

Materials and methods

Patients' tissues

A number of 41 patients with identified primary GC were enrolled in this study admitted to Zhejiang Jinhua Guangfu Tumor Hospital. The inclusive criteria were patients with pathologically diagnosed with gastric adenocarcinoma and patients receiving surgical resection. Histopathological changes of gastric tissue were evaluated in consecutive histological tissue sections stained with hematoxylin–eosin (HE). Pathological features of the HE slides were assessed by two pathologists independently. These clinical specimens and data were obtained with the institutional review board approval of Zhejiang Jinhua Guangfu Tumor Hospital, and all patients gave written informed consents.

Human cells

GC cell lines AGS (#89090402) and HGC-27 (#94042256) were from ECACC (Salisbury, UK), and human normal stomach mucosa epithelial cell line GES-1 (#BNCC337969) were from BNCC (Wuhan, China). AGS cells were cultured in Ham's F12 medium (#M15550; R&D system, Shanghai, China), and HGC-27 and GES-1 cells were cultivated in DMEM-H (#M22450; R&D system). All mediums were supplemented with 10% fetal bovine serum (#S12450H; R&D system), and all cells were incubated in a humidified sterile incubator with 5% CO_2 at 37 °C.

CircRNA characterization

RNA isolation was lysed in Trigol (#NEP019-1; Dingguo Changsheng Biotech, Beijing, China) and RNA concentration was examined by NanoDrop One/OneC (Thermo Scientific, Shanghai, China). One portion of RNAs from AGS and HGC-27 cells was disposed to 3 U/μg RNase R (Geneseed, Guangzhou, China) or equal volume of the 1 × Reaction Buffer (Geneseed) for 30 min at 37 °C. After RNase R treatment, the RNAs were directly collected for further real-time quantitative PCR (qPCR). On the other side, 4 mg/mL actinomycin D (Sigma-Aldrich, St. Louis, MO, USA) or equal volume of dimethylsulphoxide was added in cell culture medium, and RNAs of AGS and HGC-27 cells were respectively isolated after actinomycin D treatment for 0 h, 6 h, 12 h and 18 h prior to qPCR.

qPCR

One portion of RNAs from tissues and cells was reverse transcribed into complementary DNA (cDNA) at 37 °C for 60 min and 95 °C for 5 min using High capacity RNA-to-cDNA kit (#4388950; Applied Biosystem, Shanghai, China). The qPCR reaction mix was formed by adding cDNA, primers (Table 1), Luminaris HiGreen qPCR Master Mix (#K0972; Thermo Scientific), and nuclease-free water. Thermal cycling conditions were 50 °C for 2 min, 95 °C for 10 min and 40 cycles of 95 °C for 15 s and 60 °C for 60 s. The following melting curve analysis was also performed on thermal cycler. Glyceraldehyde-phosphate dehydrogenase (GAPDH) and U6 small nuclear 1 (RNU6) were detected as the correction genes, and gene expression level was calculated by $2^{-\triangle\triangle Ct}$ formula.

Cell transfection

AGS and HGC-27 cells were collected for cell transfection using Lipofectamine 2000 (Invitrogene, Carlsbad, CA, USA) per manufacturer's instructions. miRIDIAN microRNA human hsa-miR-1294 mimic and

Table 1 The qPCR primers

	Primers (5′-3′)
circFN1 (120nt)	Forward: AAGACAGCTGTTCCTCCTCC Reverse: TGAGTAACGCACCAGGAAGT
Linear FN1 (118nt)	Forward: CTGGCCAGTCCTACAACCAG Reverse: CGGGAATCTTCTCTGTCAGCC
miR-1294	Forward: GTGAGGTTGGCATTGTTG Reverse: GAACATGTCTGCGTATCTC
SIX1 (113nt)	Forward: TGCCTGGGGCAAAATGATGTA Reverse: AAAGCACAAGCAAGCCAATCC
GAPDH	Forward: GACAGTCAGCCGCATCTTCT Reverse: GCGCCCAATACGACCAAATC
RNU6	Forward: GCTTCGGCAGCACATATACTAAAAT Reverse: CGCTTCACGAATTTGCGTGTCAT

hairpin inhibitor, as well as the negative control (NC) and inhibitor NC were from Dharmacon (Lafeyette, CO, USA). RNA interference was used to silence hsa_circ_0058092 expression: hsa_circ_0058092 siRNAs (si-hsa_circ_0058092#1: targeting GGAAAAAGACAG CUGUUCCUU; si-hsa_circ_0058092#2 targeting AGA CAGCUGUUCCUCCUCCCA; si-hsa_circ_0058092#3 targeting AGGAAAAAGACAGCUGUUCCU) and hsa_circ_0058092 shRNA (sh-hsa_circ_0058092 targeting AGACAGCUGUUCCUCCUCCCA). The shRNA-pSilencer2.1-U6 hygro (AM5760; Ambion, Austin, TX, USA) was used to carry shRNA for stable cell transfection. SIX1 expression was overexpressed by transfecting recombinant pcDNA vector (#MY1012; EK-Bioscience, Shanghai, China). Transfected cells at 48 h were used in cellular assays or harvested for RNA/protein isolation.

Colony formation and EdU assay

The long-time and short-time cell proliferative abilities were respectively measured by colony formation assay and EdU staining. Cell suspension containing 250 cells were seeded in a confluent monolayer in 6-well plate and 3 replicates were set up per group. These cells were cultured for 2 weeks with culture medium changing every 3 days. Eventually, cells were fixed with 2 mL methanol for 30 min and stained with crystal violet for 20 min. Number of colonies containing more than 50 cells was counted.

Cell-Light EdU Apollo643 In Vitro Kit (Ribobio, Guangzhou, China) was employed to measure DNA synthesis capacity of differently transfected cells. Cells were pre-inoculated in 96-well plate for 24 h in triplicate, and then stained with EdU, Apollo and Hoechst33342 in sequence per manufacturer's instructions. EdU positive cell rate was reflected by the percentage of red signal (EdU positive cells) to blue signal (Hoechst positive cells).

Scratch wound assay

To determine cell migratory potential, cells were plated in a confluent monolayer in 12-well plate for 24 h, and a straight scratch was created using a sterile pipette tip with 4 replicates per group. The floating cells were removed and the remaining cells were cultured in serum-free culture mediums for 24 h. The wound image was captured at 0 h and 24 h, and relative wound closure was determined according to the change of cell-free area.

Transwell assays

Transwell assay inserts (Millipore, Billerica, MA, USA) for 24-well plate were spread with Matrigel (BD Bioscience, Franklin Lakes, NJ, USA) for cell invasion assay; matrigel-free inserts were for migration assay. The apical chamber was replenished with cell suspension containing 5×10^5 cells/well in serum-free medium, and basolateral chamber was filled with culture medium containing 10% serum as an attractant. By the way, the level of the lower medium did not reach to the lower surface of insert. Transwell systems were set in triplicate for each group cells for 48 h. Cells above the membrane of inserts were gently wiped off using cotton-tipped swabs, and the cells passed through the membrane were fixed with 2 mL methanol for 30 min, stained with crystal violet for 20 min, and observed under a microscope. Representative images from five random views were obtained at $100\times$. Migration rate and invasion rate were the percentage of purple cells with normalization to control group (as 100%).

Western blotting

Minute™ Total Protein Extraction Kit (Invent Biotechnologies, Plymouth, MN, USA) was used to isolate total protein from tissues and cells using the Denaturing Lysis Buffer (Component SD-001) for further electrophoresis using sodium dodecyl sulfate-containing polyacrylamide gel. Briefly, proteins were transferred onto nitrocellulose membranes via electrophoresis, probed with antibodies (Table 2), and developed by ECL-PLUS/Kit (GE Healthcare, Piscataway, NJ, USA). Gray density of protein bands was determined and analyzed on Quantity One software (Bio-Rad, Hercules, CA, USA). GAPDH was the protein for gray density correction. Relative protein expression was the fold change of gray density in experimental group with normalization to control group (as 1).

Bioinformatics analysis and dual-luciferase reporter system

On line starBase, circBank and CircInteractome online software were used to retrieve the miRNA binding sites in hsa_circ_0058092, and the retrieval results were showed in Venn diagram. Targetscan database was used

Table 2 The antibodies in western blotting and IHC

Antibody	Cat	Dilution ratio	Source
SIX1	10709-1-AP	1:1000/1:500	Proteintech (Wuhan, China)
E-cadherin	20874-1-AP	1:10000	Proteintech
N-cadherin	22018-1-AP	1:10000	Proteintech
GAPDH	10494-1-AP	1:50000	Proteintech
Ki67	sc-23900	1:100	Santa Cruz Biotechnology (Santa Cruz, CA, USA)
HRP-conjugated Goat Anti-Rabbit IgG (H+L)	SA00001-2	1:50000	Proteintech

to predict miR-1294-binding sites in functional gene SIX1. For luciferase reporter assay, the putative miR-1294-binding sites in hsa_circ_0058092 and 3′-untranslated region of SIX1 (SIX1 3'UTR) were mutated; then, wild-type (WT) and mutant type (MUT) of hsa_circ_0058092 and SIX1 3′UTR sequences were separately cloned into the region directly downstream of the *Firefly* luciferase gene in pmiR-Reporter vectors (Promega, Madison, WI, USA). AGS and HGC-27 cells in 96-well plate were co-transfected with 100 ng above reporter vectors, 1 ng Renilla luciferase reporter pRL-SV40 vector and 1 nM miRNA mimics. Luciferase activities were measured after transfection for 48 h using Dual-Lumi™ II Luciferase Assay Kit (Beyotime, Shanghai, China) on Microplate Luminometer (Pforzheim, Germany). *Renilla* luciferase activity was the correction for that of *Firefly*. Relative luciferase activity was the fold change of experimental activity to control group (as 1).

RNA immunoprecipitation (RIP)

RIP was carried out to validate the interaction between hsa_circ_0058092 and miR-1294. Lysates of AGS and HGC-27 cells were harvested in the RIP lysis buffer in RIP-Assay Kit (#RN1001; MBL, Woburn, MA, USA). Protein G-magnetic beads (#MJS002V2; MBL) were probed with Anti-Normal Rabbit IgG (Anti-IgG) or anti-Argonaute 2 (Anti-Ago2, #RN003M; MBL) for 4 h at 25 °C, separately; the antibody-coupled beads were incubated in cell lysates at 4 °C overnight. With Proteinase K treatment, immunoprecipitated RNAs were recovered in Trigol (Dingguo Changsheng Biotech) for qPCR.

Nude mice xenograft tumor model

A total of 12 female nude mice (BALB/C; Vital River Laboratory, Beijing, China) were seeded for xenograft experiment, and this animal experiment was authorized by the Animal Ethics Committee of Zhejiang Jinhua Guangfu Tumor Hospital. Animals feeding and operation were in compliance with the guidelines for laboratory animal welfare (GBT 35892–2018). These mice were randomly and evenly divided into 2 groups (n = 6/group), and each mouse was subcutaneously injected with 5×10^6 cells expressing sh-hsa_circ_0058092 vector or sh-NC vector into right hind flank. Subcutaneous tumors were measured every 5 days and tumor volumes were monitored; tumors were weighted and photographed at 25th day after cell injection. Animal euthanasia was performed using pentobarbital sodium anesthesia and cervical dislocation. One portion of tumors were harvested to make paraffin sections for immunohistochemistry (IHC) [24]. Antibodies in IHC were listed in Table 2

Statistical analysis

Quantitative data were presented as the mean ± standard deviation from three independent experiments. Group difference was compared using unpaired *t* test (two-tailed) and 1/2-way analysis of variance (ANOVA). Tukey's or Sidak's multiple comparison test was performed after ANOVA. Statistical analysis was performed using GraphPad Prism 8.0 (GraphPad Software, La Jolla, USA). Results were considered statistically significant at $P < 0.05$.

Results

Hsa_circ_0058092 upregulation was associated with GC

First of all, 41 GC patients were enrolled in this study and expression of hsa_circ_0058092 was substantially upregulated in these tumor tissues in contrast to paired normal tissues (Fig. 1A); Pathological alteration between tumor tissues and adjacent normal tissues was examined by HE staining (Fig. 1B). Comparing to normal GES-1 cells, AGS and HGC-27 cells showed an elevation of hsa_circ_0058092 expression (Fig. 1C). Besides, hsa_circ_0058092 expression was little affected by RNase R digestion and actinomycin D treatment (Fig. 1D–G), while expression of its linear counterpart was intensely reduced by those (Fig. 1D–G). These data indicated an upregulation of hsa_circ_0058092 in GC tissues and cells with a stable structure.

Repressing hsa_circ_0058092 functioned suppressive effect on cell proliferation and motility of GC cells in vitro

Gene manipulation of hsa_circ_0058092 was performed using siRNAs, and hsa_circ_0058092

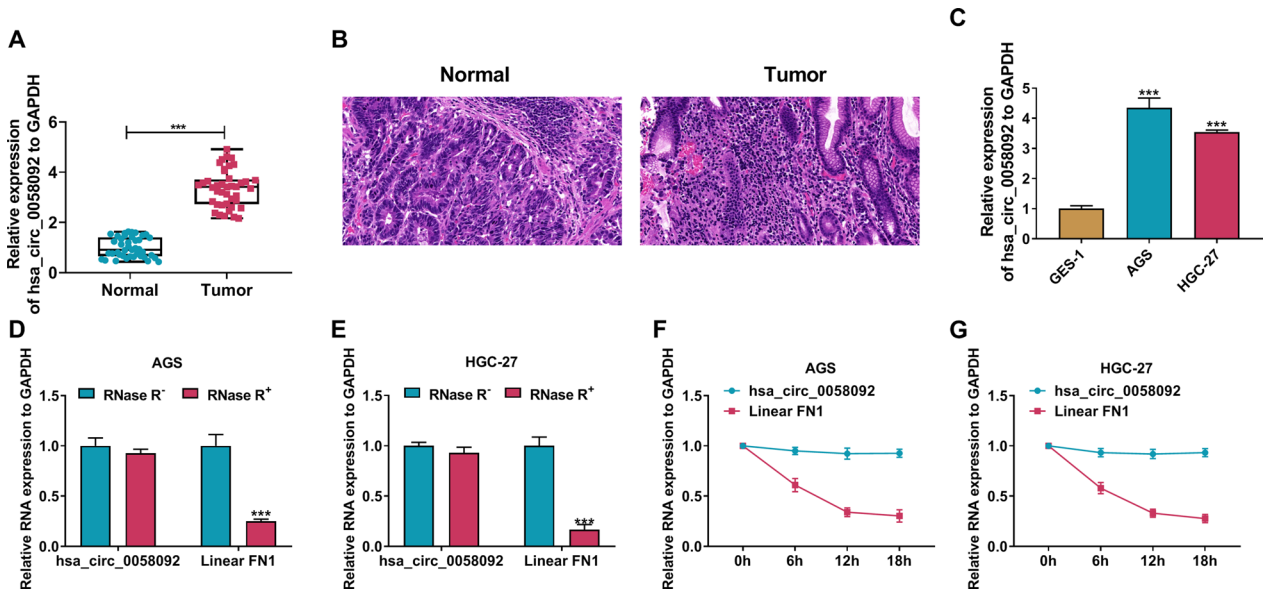

Fig. 1 Expression of hsa_circ_0058092 in GC tumor tissues and cells. **A** qPCR detected relative expression of hsa_circ_0058092 in paired tumor tissues (Tumor) and normal tissues (Normal) from 41 GC patients. **B** HE staining examined pathological alteration between Normal and Tumor samples. **C** qPCR detected relative expression of hsa_circ_0058092 in GES-1, AGS and HGC-27 cells. **D**–**G** qPCR detected relative expression of hsa_circ_0058092 and linear FN1 in (**D**, **E**) RNase R-treated (RNase R^+) and RNase R-untreated (RNase R^-) RNAs from AGS and HGC-27 cells, and (**F**, **G**) actinomycin D-treated cells for 0–18 h. ***$P < 0.001$

expression was repressed in AGS and HGC-27 cells at maximum efficiency with si-hsa_circ_0058092#2 transfection (Fig. 2A, B) Formed colony number and EdU positive cell rate of hsa_circ_0058092-interfered cells were consistently lowered than control group cells (Fig. 2C, D), suggesting an inhibiting effect of hsa_circ_0058092 depression on GC cell proliferation. Due to si-hsa_circ_0058092#2 transfection, AGS and HGC-27 cells suffered a loss of wound closure rate and transwell migration and invasion rates than cells with si-NC transfection (Fig. 2E–G), hinting a suppressive role of hsa_circ_0058092 knockdown in cell motility of GC cells. Molecularly, epithelial-mesenchymal transition (EMT)-related proteins expression was examined; expression of E-cadherin (epithelial marker) was enhanced and N-cadherin (mesenchymal marker) was inhibited in si-hsa_circ_0058092#2-transfected cells versus that in si-NC-transfected cells (Fig. 2H, I). Collectively, repressing hsa_circ_0058092 suppressed GC cell proliferation and motility in vitro.

Hsa_circ_0058092 physically interacted with miR-1294 via target binding

Nine miRNAs were predicted as computational targets for hsa_circ_0058092 (Fig. 3A), and there were five miRNAs including miR-140-3p, miR-149-5p, miR-324-5p, miR-889-3p and miR-1294 that were significantly downregulated in 6 randomly selected GC tumor tissues (Fig. 3B). In addition, only miR-140-3p and miR-1294 expression levels were highly induced in response to si-hsa_circ_0058092#2 transfection, and miR-1294 was the better sensitive one (Fig. 3C, D). Thus, miR-1294 was selected as the candidate target for hsa_circ_0058092. To further validate this target relationship, the putative binding sites of miR-1294 were mutated in hsa_circ_0058092 (Fig. 3E), and miR-1294 mimic decreased relative luciferase activity of hsa_circ_0058092 WT reporter vector in AGS and HGC-27 cells (Fig. 3F, G); however, luciferase activity of hsa_circ_0058092 MUT vector carrying site mutation could not be affected by miR-1294 (Fig. 3F, G). AGO2 is generally involved in mammalian transcriptional silencing [25], and miRNAs can direct AGO2-dependent cleavage of

(See figure on next page.)

Fig. 2 Effects of hsa_circ_0058092 knockdown on cell proliferation and motility of GC cells in vitro. AGS and HGC-27 cells were transfected with si-hsa_circ_0058092 (#1, #2 or #3) or si-NC. **A**, **B** qPCR detected relative expression of hsa_circ_0058092. **C** Colony formation assay determined the number of colonies formed in 2 weeks. **D** EdU assay measured EdU positive cell rate (%) in Hoechst positive cells. **E** Scratch wound assay displayed relative wound closure (%) after 24 h. **F**, **G** Transwell assays tested migration rate (%) and invasion rate (%) after 24 h. **H**, **I** Western blotting detected relative protein expression of E-cadherin and N-cadherin with correction to GAPDH. **$P < 0.01$ and ***$P < 0.001$

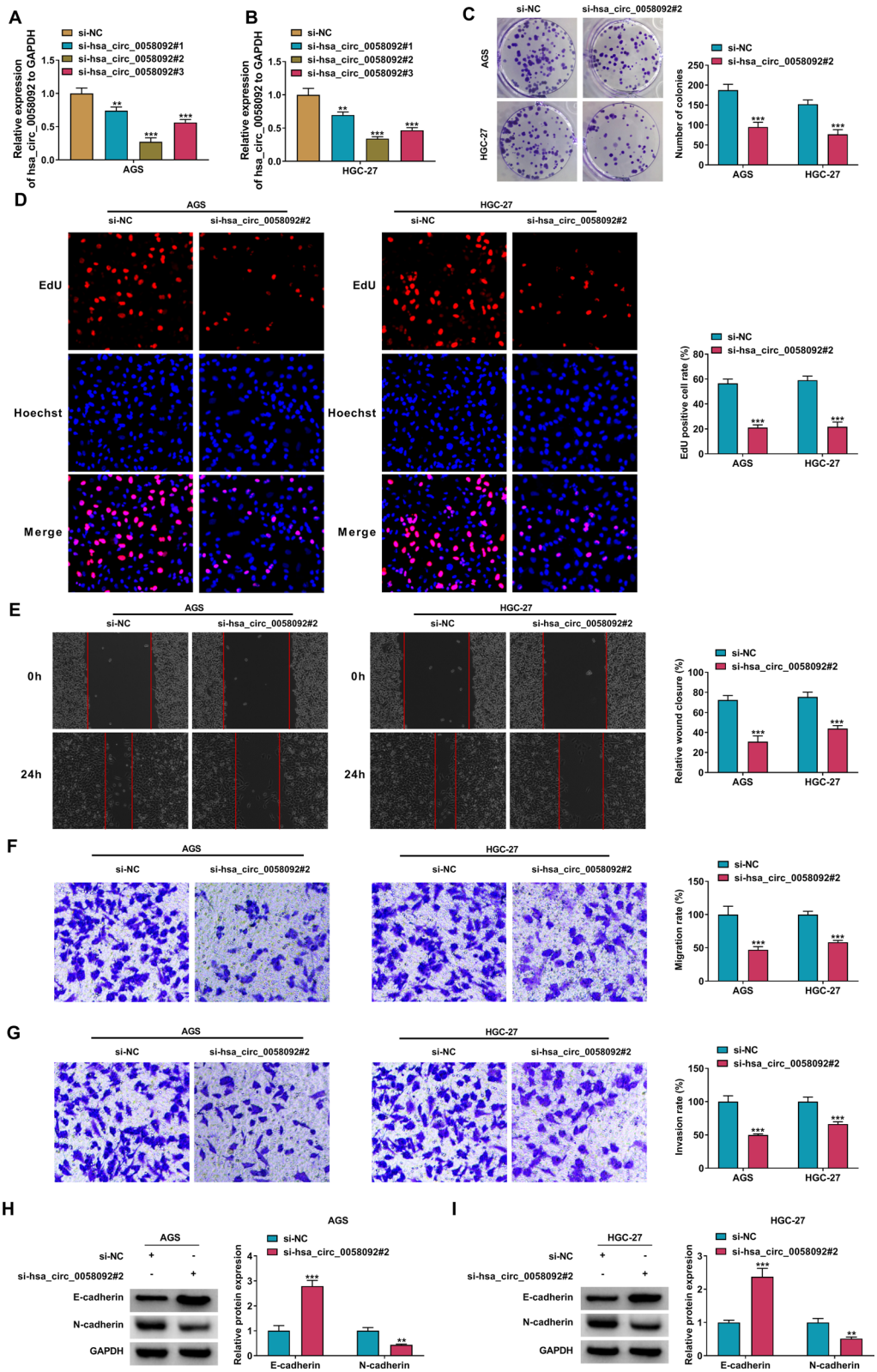

Fig. 2 (See legend on previous page.)

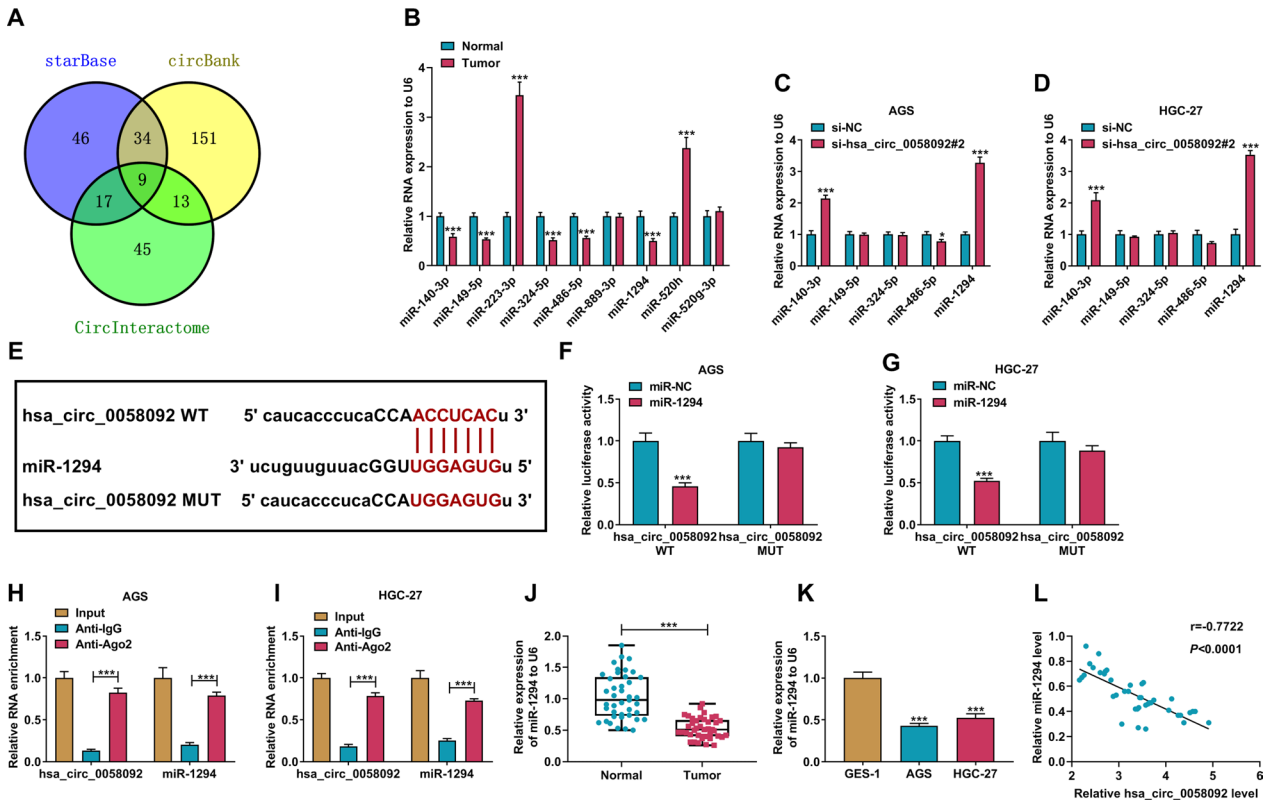

Fig. 3 Physical interaction between hsa_circ_0058092 and miR-1294. **A** Venn diagram showed the number of miRNAs that were predicted as targets for hsa_circ_0058092 in starBase, circBank and CircInteractome online software. **B**–**D** qPCR examined relative expression of (**B**) miR-140-3p, miR-149-5p, miR-223-3p, miR-324-5p, miR-486-5p, miR-889-3p, miR-1294, miR-520 h, and miR-520 g-3p in 6 pairs of randomly selected Normal and Tumor tissues, and (**C**, **D**) miR-140-3p, miR-149-5p, miR-324-5p, miR-486-5p, and miR-1294 in AGS and HGC-27 cells transfected with si-hsa_circ_0058092 (#2) or si-NC. (**E**) Schematic diagram showed the wild-type and mutations of the predicted miR-1294-binding sites in hsa_circ_0058092 WT and MUT. (**F**, **G**) Dual-luciferase reporter assay determined relative luciferase activity of hsa_circ_0058092 WT and MUT reporter vectors in response to miR-1294 mimic (miR-1294) or miR-NC mimic (miR-NC) in AGS and HGC-27 cells. **H**, **I** RIP assay testified relative RNA enrichment of hsa_circ_0058092 and miR-1294 in the Input, Anti-IgG group and Anti-Ago2 group in cell lysate of AGS and HGC-27 cells. **J**, **K** qPCR examined relative expression of miR-1294 in **J** 41 pairs of Normal and Tumor tissues, and **K** GES-1, AGS and HGC-27 cells. **L** Pearson's correlation coefficient was determined between relative hsa_circ_0058092 and miR-1294 levels in 41 Tumor tissues. ***$P < 0.001$

circRNAs and mRNAs in an RNA interference-like manner [26, 27]. Moreover, hsa_circ_0058092 and miR-1294 were markedly co-enriched in Anti-Ago2-mediated RIP with comparing to that mediated by Anti-IgG (Fig. 3H, I). Expression of miR-1294 was downregulated in both GC tumor tissues and cells (AGS and HGC-27) than normal ones (Fig. 3J, K). More intriguingly, relative miR-1294 level in these GC tumors was inversely and linearly correlated with hsa_circ_0058092 level (Fig. 3L). These findings showed a direct target relationship between hsa_circ_0058092 and miR-1294, and the both expression was closely correlated with each other in GC tumor.

Inhibiting miR-1294 was detrimental to the anti-tumor role of hsa_circ_0058092 knockdown in GC cells

Inhibitor of miR-1294 rendered the silencing of miR-1294 in AGS and HGC-27 cells (Fig. 4A, B), and miR-1294 silencing caused an improvement of colony number and EdU positive rate in hsa_circ_0058092-depressed cells (Fig. 4C–F). The suppression of si-hsa_circ_0058092#2 sole transfection on wound closure and transwell migration rate of AGS and HGC-27 cells was attenuated by co-transfecting si-hsa_circ_0058092#2 and miR-1294-5p inhibitor (Fig. 4G–J). Besides, invasion ability of AGS and HGC-27 cells was reduced in condition of hsa_circ_0058092 depression, however this regulatory effect was partially abated when miR-1294 was synchronously blocked, as described by the rescue of transwell invasion rate and N-cadherin expression, and the exhaustion of E-cadherin expression (Fig. 4K–N). These results demonstrated a detrimental effect of miR-1294 inhibition on the roles of hsa_circ_0058092 knockdown in GC cell proliferation and motility in vitro.

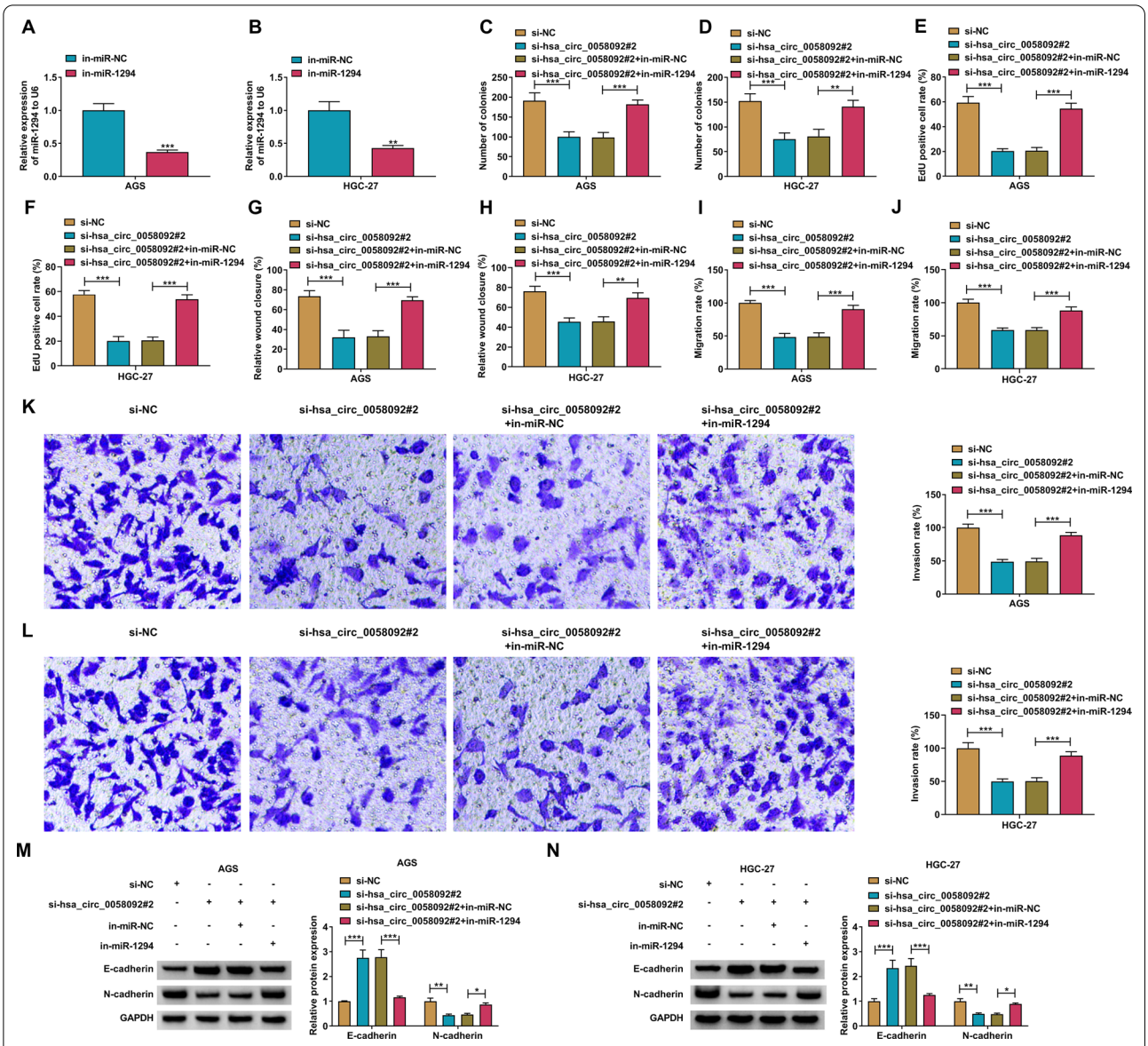

Fig. 4 Interactive role between hsa_circ_0058092 depression and miR-1294 inhibition in GC cells. **A**, **B** qPCR examined relative expression of miR-1294 in AGS and HGC-27 cells transfected with miR-1294 inhibitor (in-miR-1294) or miR-NC inhibitor (in-miR-NC). **C**–**N** AGS and HGC-27 cells transfected with si-hsa_circ_0058092 (#2) or si-NC, si-hsa_circ_0058092 (#2) along with in-miR-1294 or in-miR-NC. **C**, **D** Colony formation assay determined the number of colonies formed in 2 weeks. **E**, **F** EdU assay measured EdU positive cell rate (%) in Hoechst positive cells. **G**, **H** Scratch wound assay displayed relative wound closure (%) after 24 h. **I**–**L** Transwell assays tested (**I**, **J**) migration rate (%) and (**K**, **L**) invasion rate (%) after 24 h. **M**, **N** Western blotting detected relative protein expression of E-cadherin and N-cadherin with correction to GAPDH. *$P < 0.05$, **$P < 0.01$ and ***$P < 0.001$

MiR-1294 directly interacted with SIX1 via targeting

By retrieving bioinformatics database, SIX1 was an unidentified target gene for miR-1294, and the response elements between both were showed (Fig. 5A). Dual-luciferase reporter assay further identified the responsiveness of miR-1294 mimic to SIX 3'UTR WT reporter vector instead of the MUT vector (Fig. 5B, C). Expression of SIX1 at mRNA and protein levels was substantially increased in GC patients' tumor tissues (Fig. 5D, G); notably, SIX1 mRNA level was negatively correlated with miR-1294 level and positively correlated with hsa_circ_0058092 level (Fig. 5E, F). In vitro GC cells, SIX1 expression levels were higher in AGS and HGC-27 cells than normal GES-1 cells (Fig. 5H, I). Additionally, si-hsa_circ_0058092#2 transfection resulted in SIX1 downregulation, and miR-1294 inhibitor co-transfection

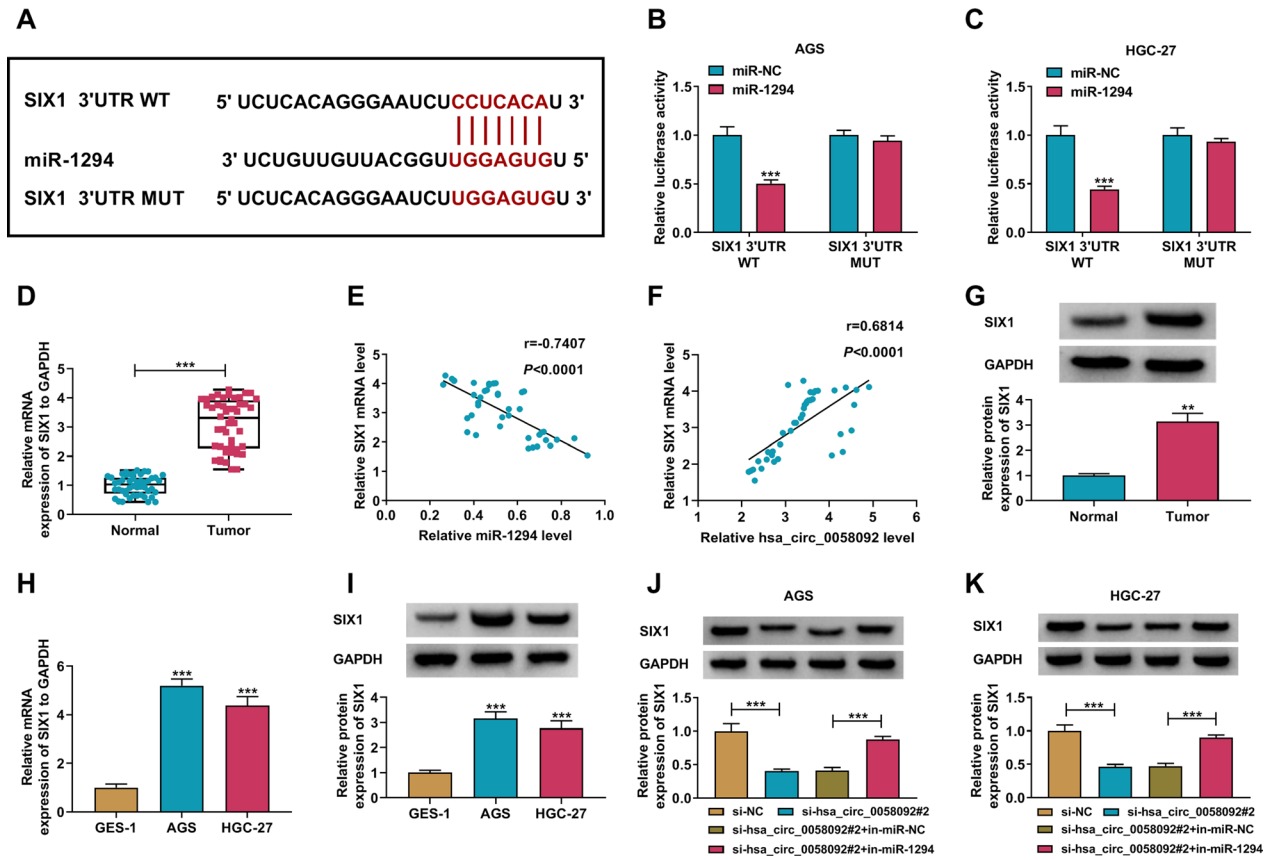

Fig. 5 Physical interaction between miR-1294 and SIX1. **A** Schematic diagram showed the wild-type and mutations of the predicted miR-1294-binding sites in SIX1 3′UTR WT and MUT. **B**, **C** Dual-luciferase reporter assay determined relative luciferase activity of SIX13′UTR WT and MUT reporter vectors in response to miR-1294 or miR-NC in AGS and HGC-27 cells. **D** qPCR examined relative mRNA expression of SIX1 in **J** 41 pairs of Normal and Tumor tissues. **E**, **F** Pearson's correlation coefficient was determined between relative SIX1 mRNA level and miR-1294 and hsa_circ_0058092 levels in 41 Tumor tissues. **G** Western blotting examined relative protein expression of SIX1 in one pair of randomly selected Normal and Tumor tissues. **H**, **I** qPCR and western blotting detected relative mRNA and protein expression of SIX1 in GES-1, AGS and HGC-27 cells. **J**, **K** Western blotting measured relative protein expression of SIX1 in AGS and HGC-27 cells transfected with si-hsa_circ_0058092 (#2) or si-NC, si-hsa_circ_0058092 (#2) along with in-miR-1294 or in-miR-NC. $^{**}P < 0.01$ and $^{***}P < 0.001$

diminished the regulatory effect of hsa_circ_0058092 knockdown on SIX1 protein expression (Fig. 5J, K). These outcomes declared a direct target relationship between miR-1294 and SIX1, and a close association among hsa_circ_0058092, miR-1294 and SIX1 expression in GC.

Reinforcing SIX1 was prejudicial to the integrated anti-proliferation and anti-motility role of miR-1294 overexpression in GC cells

Mimic of miR-1294 caused overexpression of miR-1294 in AGS and HGC-27 cells (Fig. 6A), and similarly SIX1 overexpression vector induced the ectopic expression of SIX1 (Fig. 6B). Formed colony number in AGS and HGC-27 cells and EdU positive rate were consistently declined in solely miR-1294 mimic-transfected cells (Fig. 6C–F), and this decline was partially abrogated with SIX1 vector co-transfection (Fig. 6C–F). Reinforcing miR-1294 suppressed wound closure and transwell migration rate of AGS and HGC-27 cells, which was attenuated by restoring SIX1 (Fig. 6G–J); besides, transwell invasion rate and N-cadherin expression in AGS and HGC-27 cells were reduced in the presence of miR-1294 mimic (Fig. 6K–N); however these regulatory effects were mitigated by introducing SIX1 vector (Fig. 6K–N). These results depicted a suppressive role of miR-1294 overexpression in GC cell proliferation and motility in vitro, and a detrimental effect of SIX1 upregulation on the role of miR-1294 overexpression.

Blocking hsa_circ_0058092 restricted the tumorigenicity of GC cells in vivo

AGS cells stably expressing sh-hsa_circ_0058092 or sh-NC were used to induce xenograft tumors in nude mice, and tumors were formed in both group

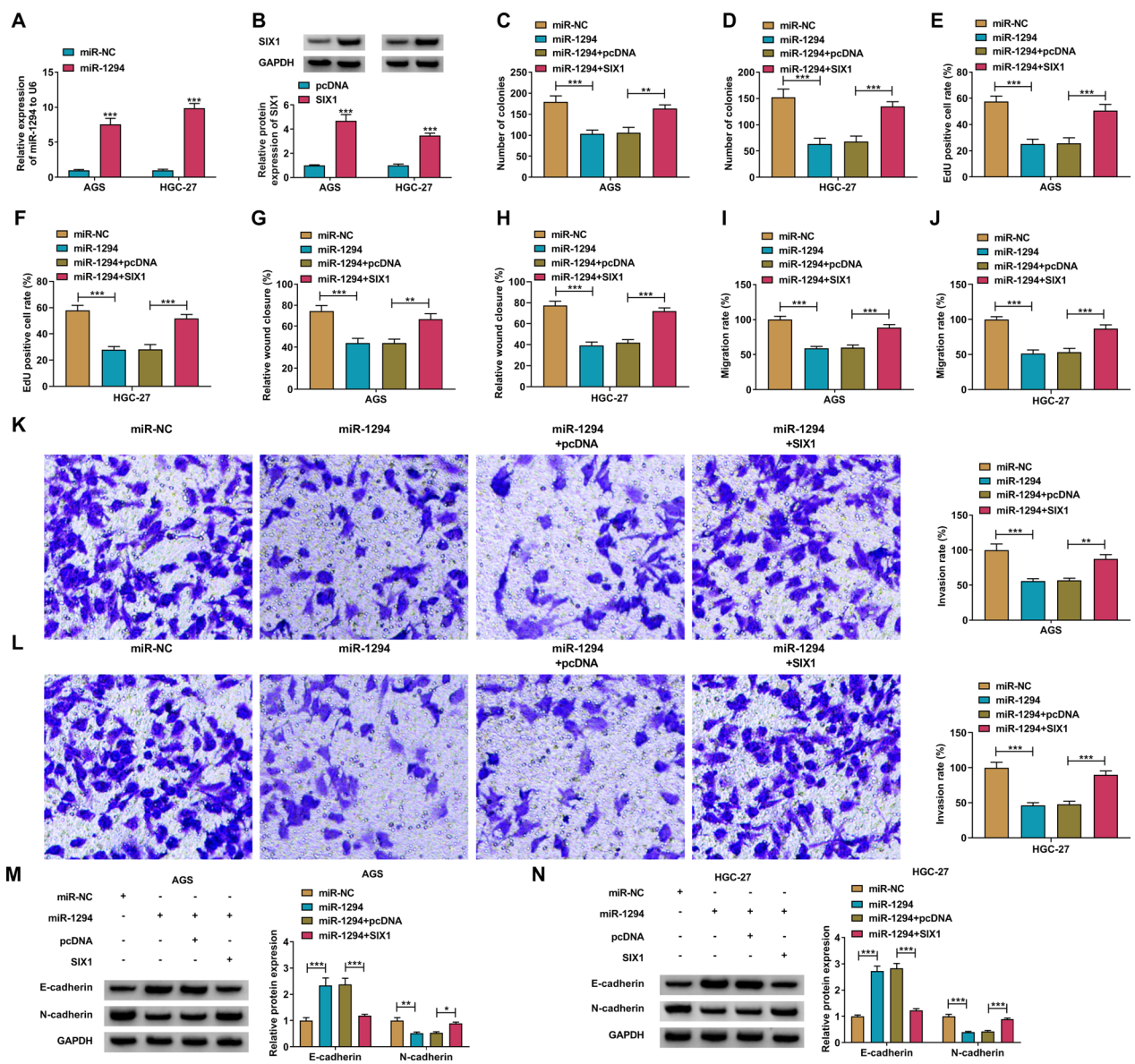

Fig. 6 Reciprocal impact between miR-1294 overexpression and SIX1 hyperexpression in proliferation and motility of GC cells. **A**, **B** qPCR and western blotting examined **A** relative expression of miR-1294 and **B** relative protein expression of SIX1 in AGS and HGC-27 cells transfected with miR-1294 or miR-NC, pcDNA-SIX1 vector (SIX1) or pcDNA empty vector (pcDNA). **C**–**N** AGS and HGC-27 cells transfected with miR-1294 or miR-NC, miR-1294 along with SIX1 vector or pcDNA vector. **C**, **D** Colony formation assay determined the number of colonies formed in 2 weeks. **E**, **F** EdU assay measured EdU positive cell rate (%) in Hoechst positive cells. **G**, **H** Scratch wound assay displayed relative wound closure rate after 24 h. **I**–**L** Transwell assays tested **I**, **J** migration rate (%) and **K**, **L** invasion rate (%) after 24 h. **M**, **N** Western blotting detected relative protein expression of E-cadherin and N-cadherin with correction to GAPDH. *$P < 0.05$, **$P < 0.01$ and ***$P < 0.001$

(Fig. 7A); nevertheless, tumor volume and weight in sh-hsa_circ_0058092 group were overall smaller than sh-NC group (Fig. 7B, C). Molecularly, sh-hsa_circ_0058092 group tumors exhibited a downregulation of hsa_circ_0058092 and SIX1 (Fig. 7D, F and G) and an upregulation of miR-1294 (Fig. 7E). Furthermore, the delayed tumors in sh-hsa_circ_0058092 group was allied with less SIX1-positive cells and ki-67-positive cells (Fig. 7H, I). Expression of E-cadherin was promoted and N-cadherin was inhibited in tumor tissues expressing sh-hsa_circ_0058092 (Fig. 7J). These data revealed that blocking hsa_circ_0058092 might restrict GC tumor growth and motility in vivo with regulation of miR-1294 and SIX1.

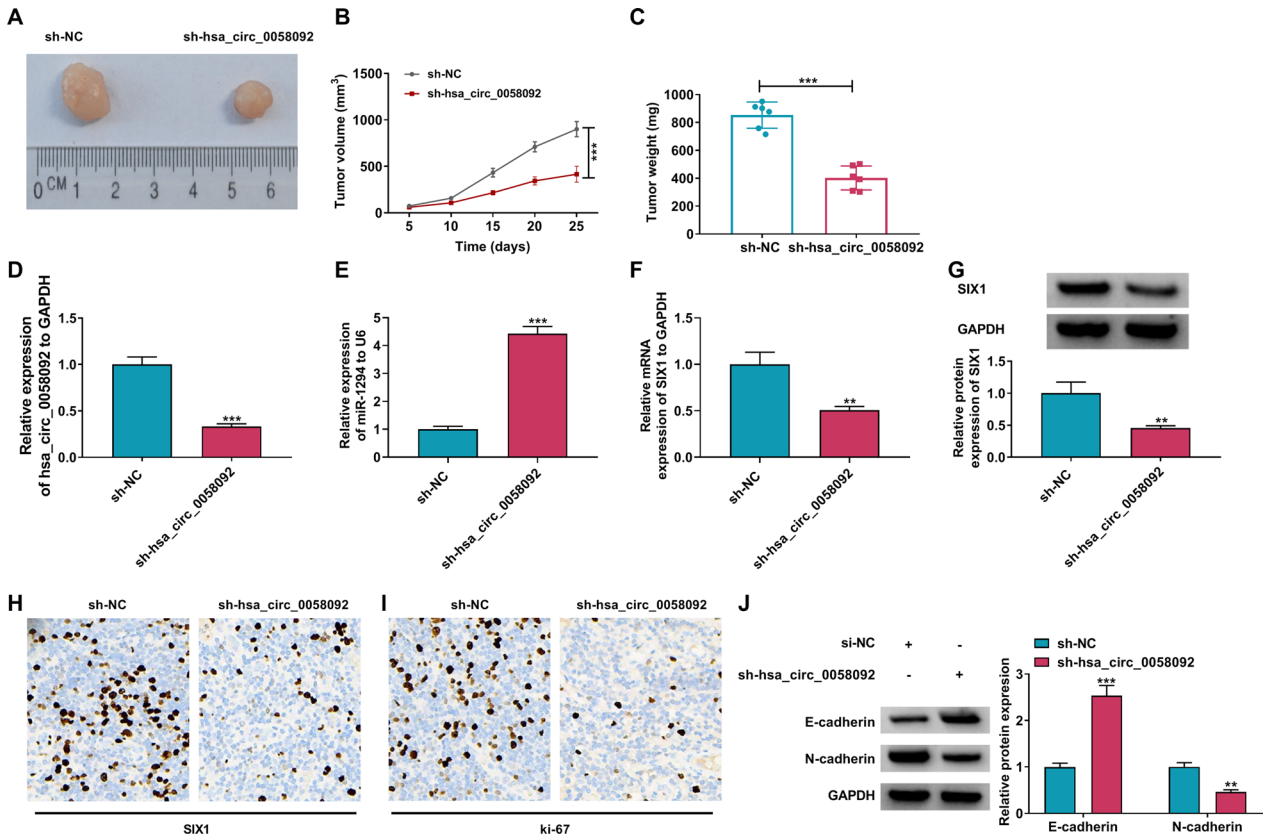

Fig. 7 Role of blocking hsa_circ_0058092 in tumorigenicity of GC cells in vivo. AGS cells stably expressing sh-hsa_circ_0058092 or sh-NC were used to induce xenograft tumors in nude mice (n = 6). **A** Xenograft tumors were excised and photographed, and the most representative tumors were presented. **B** Tumor volume was monitored at an interval of every 5 days after cell injection. **C** Tumor weight was determined after photographing. **D**–**F** qPCR detected relative expression of hsa_circ_0058092, miR-1294 and SIX1 mRNA, and **G**, **J** western blotting measured relative protein expression of SIX1, E-cadherin and N-cadherin, and **H**, **I** IHC examined in situ expression of SIX1 and ki-67 in xenograft tumor tissues

Discussion

FN1 transcript could generate different circRNAs via back-splicing. For example, overexpression of hsa_circ_0058147 originating from exons 10–12 of FN1 could enhance cisplatin resistance in GC cells, and meanwhile its silencing could reverse cisplatin resistance in the cisplatin-resistant GC cells by regulating cell viability and apoptosis [28]. Exons 15–19 of FN1-derived circRNA hsa_circ_0058124 was declared to contribute to sorafenib resistance in hepatocellular carcinoma both in vitro and in vivo [29]. Hsa_circ_0058092 described in this study was originated from FN1 exons 26–39 and was the most upregulated circRNA in GC tumors according to NGS data [16]. However, Bu et al. [16] showed that hsa_circ_0058092 might control metabolism of GC cells via miR-4269/PODXL axis by functional analysis and miRNA binding site prediction [16]; they did not further validate above results via experiments. Here, the present work was the first one to reveal the mechanism of hsa_circ_0058092 in GC cell proliferation, migration and invasion, and the results showed that hsa_circ_0058092 modulated GC cell malignancy through the miR-1294/SIX1 axis.

qPCR data showed that hsa_circ_0058092 expression was substantially higher in GC tumors, which was in favor with previous NGS data [16]. Besides, hsa_circ_0058092 was resistant to RNase R digestion and actinomycin D treatment, and this outcome validated the closed-loop structure and structure stability of hsa_circ_0058092. Functionally, we noticed that inhibiting hsa_circ_0058092 overall suppressed colony formation, cell proliferation, wound closure, EMT, migration and invasion of GC cells, as well as tumor growth in xenograft nude mice. These results might reveal an integrated anti-proliferation and anti-motility role of hsa_circ_0058092 downregulation in GC, suggesting that hsa_circ_0058092 was an oncogene, and inhibiting hsa_circ_0058092 could be a potential therapeutic therapy for GC development. By the way, hsa_circ_0058092 was also reported to protect endothelial progenitor cell functions including

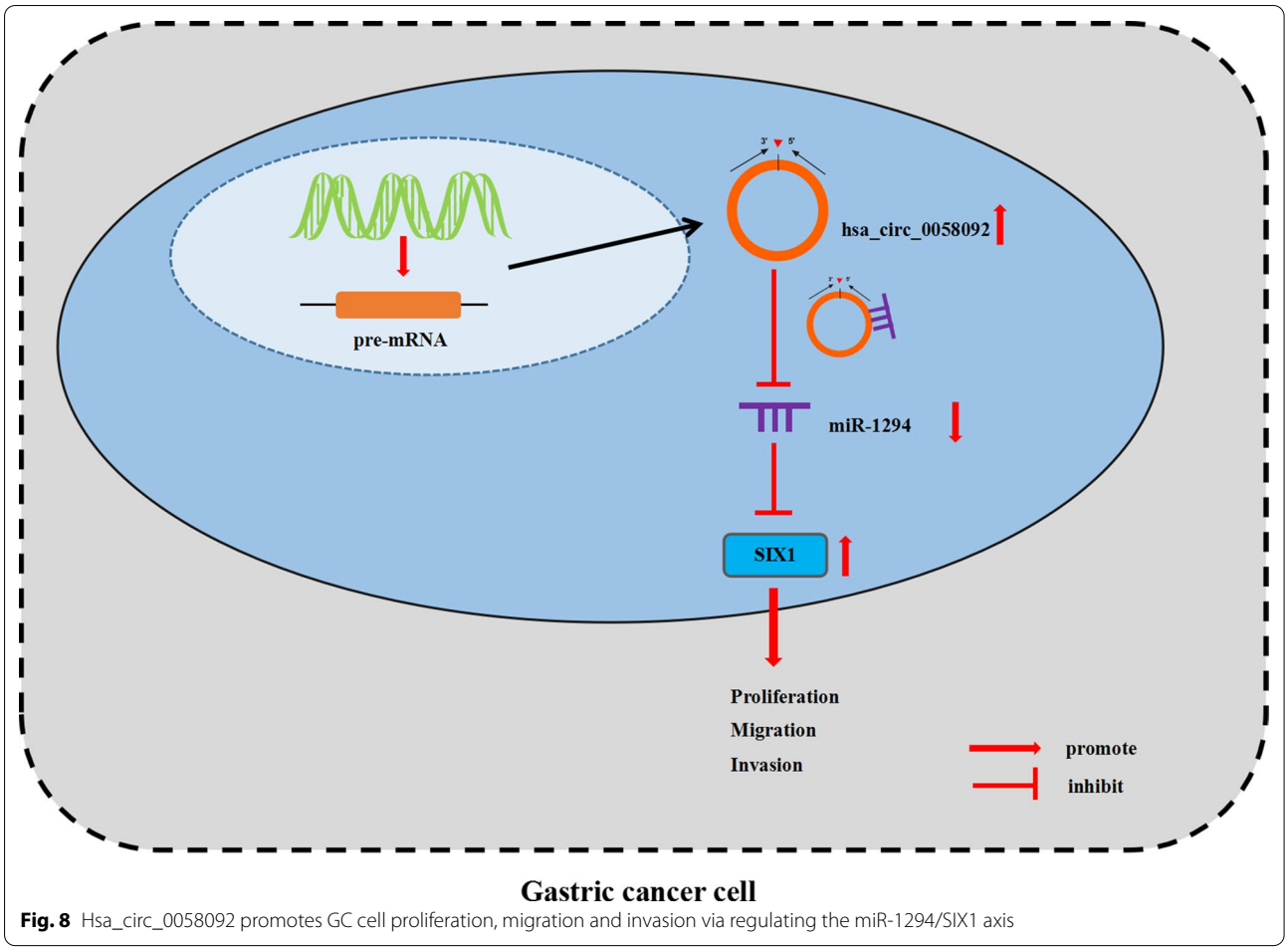

Fig. 8 Hsa_circ_0058092 promotes GC cell proliferation, migration and invasion via regulating the miR-1294/SIX1 axis

proliferation, migration and angiogenic differentiation under hyperglycemia condition [30]. Taken together, hsa_circ_0058092 might be a versatile circRNA in human diseases. Target gene prediction was performed using different databases in this study. As a result, we found that dual-miRNAs including miR-140-3p and miR-1294 were potential targets for hsa_circ_0058092, and the both miRNAs were GC-related [21, 31]. Herein, miR-1294 was locked as hsa_circ_0058092 target for further validation, since miR-1294 expression was more sensitive to hsa_circ_0058092 silencing in GC cells. At the same time, the potential association between hsa_circ_0058092 and miR-140-3p was left to be further functionally confirmed.

In this study, expression of miR-1294 was distinctively downregulated in GC tumors and its expression was moderately correlated with hsa_circ_0058092 level. The downregulation of miR-1294 in this cohort of GC patients supported previous findings [21, 32, 33]. Higher miR-1294 level showed a significant longer disease-free survival and overall survival, as well as less metastasis [21, 32]. Our data displayed an inhibitory effect of miR-1294 overexpression on GC cell proliferation and motility; blocking miR-1294 recovered GC tumor cell behaviors under hsa_circ_0058092 knockdown condition, which was similar to the rescue effect of miR-1294 inhibitor in NEAT1-silenced GC cells [33]. Besides, the finding that miR-1294 upregulation was detrimental to EMT, invasion and wound closure in GC cells was in favor of Wang et al. [32]. Here, SIX1 was predicted and verified as a novel target functional gene for miR-1294. We observed an upregulation of SIX1 in GC tumors and cells, which was in agreement with former literatures [23, 34–36]. Functionally, SIX1 was associated with cell proliferation and motility of GC cells. Additionally, SIX1 depression played versatile roles in GC cells, such as promoting 5-Fluorouracil sensitivity and triggering mitochondrial apoptosis [35].

Transcription factor CEBPB might be a direct regulator in the transcription of hsa_circ_0058092 [16]. However, whether there was a binding site of transcription factor SIX1 in genome region of hsa_circ_0058092 was unsolved yet, and this hypothesis was worthy of study.

Previously, clinical significance of hsa_circ_0058092 had been demonstrated in a group of GC patients, and hsa_circ_0058092 expression might predict high invasion degree and poor overall survival [16]. While, this study did not identify the clinical values of hsa_circ_0058092 expression in tumor tissues in clinicopathological factors of this cohort of GC patients including TNM stage, lymph node metastasis and prognosis. Particularly worth mentioning was that this research direction could be further carried out later to measure whether blood/tissue hsa_circ_0058092 could be a biomarker for the diagnosis and prognosis of GC, just like the existing biomarkers hsa_circ_0001811 and hsa_circ_000067582 [37, 38]. KEGG pathway analysis suggested the association between hsa_circ_0058092/miRNAs/mRNAs and metabolic processes [16]. Apart from metabolism transforming [39], chemoresistance is also closely related to the occurrence, progression and poor prognosis of GC [40]. However, whether hsa_circ_0058092 could be implicated in the two phenotypic transformations of GC remains to be further figured out.

All in all, we discovered an upregulation of hsa_circ_0058092 and SIX1 in GC patients' tumors and cells, accompanied with miR-1294 downregulation. Moreover, inhibiting hsa_circ_0058092/miR-1294 axis could suppress cell proliferation and motility of GC cells in regulation of SIX1 expression. Hsa_circ_0058092/miR-1294/SIX1 axis might be a novel ceRNA regulatory mechanism underlying GC tumorigenesis (Fig. 8). Target inhibiting hsa_circ_0058092 might be a potential therapeutic approach in GC.

Acknowledgements
None

Author contributions
Jianming Fang performed experiments, analyzed data, and wrote the manuscript. Xiaodong Zhang designed research, performed experiments, and analyzed data. Jianxin Huang collected data and operated the software. All authors read and approved the final manuscript.

Funding
None.

Availability of data and materials
The data sets used and/or analyzed during the current study are available from the corresponding author on reasonable request.

Declarations

Competing interests
The authors declare that they have no competing interests.

Received: 8 April 2022 Accepted: 17 June 2022
Published online: 08 July 2022

References

1. Bray F, Ferlay J, Soerjomataram I, Siegel RL, Torre LA, Jemal A (2018) Global cancer statistics 2018: GLOBOCAN estimates of incidence and mortality worldwide for 36 cancers in 185 countries. CA Cancer J Clin 68(6):394–424
2. Smyth EC, Nilsson M, Grabsch HI, van Grieken NC, Lordick F (2020) Gastric cancer. Lancet 396(10251):635–648
3. Zhang X, Li M, Chen S et al (2018) Endoscopic screening in Asian countries is associated with reduced gastric cancer mortality: a meta-analysis and systematic review. Gastroenterology 155(2):347-354 e349
4. Levy I, Gralnek IM (2016) Complications of diagnostic colonoscopy, upper endoscopy, and enteroscopy. Best Pract Res Clin Gastroenterol 30(5):705–718
5. Li Z, Ruan Y, Zhang H, Shen Y, Li T, Xiao B (2019) Tumor-suppressive circular RNAs: mechanisms underlying their suppression of tumor occurrence and use as therapeutic targets. Cancer Sci 110(12):3630–3638
6. Lu Y, Li Z, Lin C, Zhang J, Shen Z (2021) Translation role of circRNAs in cancers. J Clin Lab Anal 35(7):e23866
7. Jiao S, Wu S, Huang S, Liu M, Gao B (2021) Advances in the identification of circular RNAs and research into circRNAs in human diseases. Front Genet 12:665233
8. Wu W, Zhen T, Yu J, Yang Q (2020) Circular RNAs as new regulators in gastric cancer: diagnosis and cancer therapy. Front Oncol 10:1526
9. Shan C, Zhang Y, Hao X, Gao J, Chen X, Wang K (2019) Biogenesis, functions and clinical significance of circRNAs in gastric cancer. Mol Cancer 18(1):136
10. Necula L, Matei L, Dragu D et al (2019) Recent advances in gastric cancer early diagnosis. World J Gastroenterol 25(17):2029–2044
11. Li L, Zhu Z, Zhao Y et al (2019) FN1, SPARC, and SERPINE1 are highly expressed and significantly related to a poor prognosis of gastric adenocarcinoma revealed by microarray and bioinformatics. Sci Rep 9(1):7827
12. Tian Y, Xing Y, Zhang Z, Peng R, Zhang L, Sun Y (2020) Bioinformatics analysis of key genes and circRNA-miRNA-mRNA regulatory network in gastric cancer. Biomed Res Int 2020:2862701
13. Wang C, Huang Y, Zhang J, Fang Y (2020) MiRNA-339-5p suppresses the malignant development of gastric cancer via targeting ALKBH1. Exp Mol Pathol 115:104449
14. Liu X, Xu D, Xu X, Xue Q, Gao X, Tang C (2021) MiR-216b regulates the tumorigenesis of gastric cancer by targeting PXN. Pathol Res Pract 218:153325
15. Verma R, Sharma PC (2018) Next generation sequencing-based emerging trends in molecular biology of gastric cancer. Am J Cancer Res 8(2):207–225
16. Bu X, Zhang X, Luan W et al (2020) Next-generation sequencing reveals hsa_circ_0058092 being a potential oncogene candidate involved in gastric cancer. Gene 726:144176
17. Ma C, Wang X, Yang F et al (2020) Circular RNA hsa_circ_0004872 inhibits gastric cancer progression via the miR-224/Smad4/ADAR1 successive regulatory circuit. Mol Cancer 19(1):157–157
18. Yu T, Ran L, Zhao H et al (2021) Circular RNA circ-TNPO3 suppresses metastasis of GC by acting as a protein decoy for IGF_2BP_3 to regulate the expression of MYC and SNAIL. Mol Ther Nucleic Acids 26:649–664
19. Li C, Tian Y, Liang Y, Li Q (2020) Circ_0008035 contributes to cell proliferation and inhibits apoptosis and ferroptosis in gastric cancer via miR-599/EIF4A1 axis. Cancer cell Int 20:84
20. He S, Du W, Li M, Yan M, Zheng F (2020) PODXL might be a new prognostic biomarker in various cancers: a meta-analysis and sequential verification with TCGA datasets. BMC Cancer 20(1):620
21. Shi YX, Ye BL, Hu BR, Ruan XJ (2018) Expression of miR-1294 is downregulated and predicts a poor prognosis in gastric cancer. Eur Rev Med Pharmacol Sci 22(17):5525–5530
22. Wu W, Ren Z, Li P et al (2015) Six1: a critical transcription factor in tumorigenesis. Int J Cancer 136(6):1245–1253
23. Lv H, Cui A, Sun F et al (2014) Sineoculis homeobox homolog 1 protein as an independent biomarker for gastric adenocarcinoma. Exp Mol Pathol 97(1):74–80
24. Liu H, Lu J, Hua Y et al (2015) Targeting heat-shock protein 90 with ganetespib for molecularly targeted therapy of gastric cancer. Cell Death Dis 6:e1595

25. Janowski BA, Huffman KE, Schwartz JC et al (2006) Involvement of AGO_1 and AGO_2 in mammalian transcriptional silencing. Nat Struct Mol Biol 13(9):787–792
26. Hansen TB, Wiklund ED, Bramsen JB et al (2011) miRNA-dependent gene silencing involving Ago2-mediated cleavage of a circular antisense RNA. EMBO J 30(21):4414–4422
27. Yekta S, Shih IH, Bartel DP (2004) MicroRNA-directed cleavage of HOXB8 mRNA. Science 304(5670):594–596
28. Huang XX, Zhang Q, Hu H et al (2020) A novel circular RNA circFN1 enhances cisplatin resistance in gastric cancer via sponging miR-182–5p. J Cell Biochem. https://doi.org/10.1002/jcb.29641
29. Yang C, Dong Z, Hong H et al (2020) circFN1 Mediates sorafenib resistance of hepatocellular carcinoma cells by sponging miR-1205 and regulating E_2F_1 expression. Mol Ther Nucleic Acids 22:421–433
30. Cheng J, Hu W, Zheng F, Wu Y, Li M (2020) hsa_circ_0058092 protects against hyperglycemiainduced endothelial progenitor cell damage via miR217/FOXO3. Int J Mol Med 46(3):1146–1154
31. Zhang L, Chang X, Zhai T et al (2020) A novel circular RNA, circ-ATAD1, contributes to gastric cancer cell progression by targeting miR-140-3p/YY1/PCIF1 signaling axis. Biochem Biophys Res Commun 525(4):841–849
32. Wang Y, Liu G, Sun S, Qin J (2020) miR-1294 alleviates epithelial-mesenchymal transition by repressing FOXK1 in gastric cancer. Genes Genomics 42(2):217–224
33. Wu D, Li H, Wang J et al (2020) LncRNA NEAT1 promotes gastric cancer progression via miR-1294/AKT1 axis. Open Med (Wars) 15(1):1028–1038
34. Emadi-Baygi M, Nikpour P, Emadi-Andani E (2015) SIX1 overexpression in diffuse-type and grade III gastric tumors: features that are associated with poor prognosis. Adv Biomed Res 4:139
35. Du P, Zhao J, Wang J et al (2017) Sine oculis homeobox homolog 1 regulates mitochondrial apoptosis pathway via caspase-7 in gastric cancer cells. J Cancer 8(4):636–645
36. Xie Y, Jin P, Sun X et al (2018) SIX_1 is upregulated in gastric cancer and regulates proliferation and invasion by targeting the ERK pathway and promoting epithelial-mesenchymal transition. Cell Biochem Funct 36(8):413–419
37. Zhang H, Li Z, Ruan Y, Sun W, Yu R (2021) Low expression of hsa_circ_0001811 in gastric cancer and its role in clinical diagnosis. J Clin Lab Anal 35(2):e23642
38. Yu X, Ding H, Yang L et al (2020) Reduced expression of circRNA hsa_circ_0067582 in human gastric cancer and its potential diagnostic values. J Clin Lab Anal 34(3):e23080
39. Liu Y, Zhang Z, Wang J et al (2019) Metabolic reprogramming results in abnormal glycolysis in gastric cancer: a review. Onco Targets Ther 12:1195–1204
40. Marin JJG, Perez-Silva L, Macias RIR et al (2020) Molecular bases of mechanisms accounting for drug resistance in gastric adenocarcinoma. Cancers (Basel) 12(8):2116

Publisher's Note